

- ◉ Precision Spectral Pyranometer
- Manufacturer's Photovoltaic Sensor

**Figure 1 NIST's Photovoltaic System**

Each PV assembly is laminated to 51 mm high spacers that are in turn laminated to 51 mm thick sheets of extruded polystyrene insulation, Fig. 2. The extruded polystyrene insulation provides additional insulation, approximately 1.76 m<sup>2</sup> K/W (R-10 °F·ft<sup>2</sup>·h/Btu), to the portion of the roof covered by the photovoltaic modules. The insulation pieces are interlocked with surrounding pieces by means of a “tongue and groove” system.

The outer photovoltaic module assemblies are secured by means of a concrete ballast system. This mounting system results in an assembly that can resist the uplifting forces of wind and eliminates the need for roofing penetrations. Based upon wind tunnel tests and subsequent calculations commissioned by the manufacturer [1], the design can withstand a 3-second 63 m/s (140 mph) wind gust. For the particular NIST installation, the design condition is a 3-second wind gust of 45 m/s (100 mph) [2].

According to the photovoltaic module manufacturer [3], each module produces 150 watts at standard rating conditions (1000 W/m<sup>2</sup>, 25°C, and an absolute air mass value of 1.5). The 234 modules are electrically connected to form 18 strings, each string consisting of 13 modules in series. The eighteen strings are electrically connected in parallel. At standard rating conditions the photovoltaic array can produce 35 kW of direct current electrical power. Table 1 summarizes the electrical specifications associated with an individual module and the entire array.

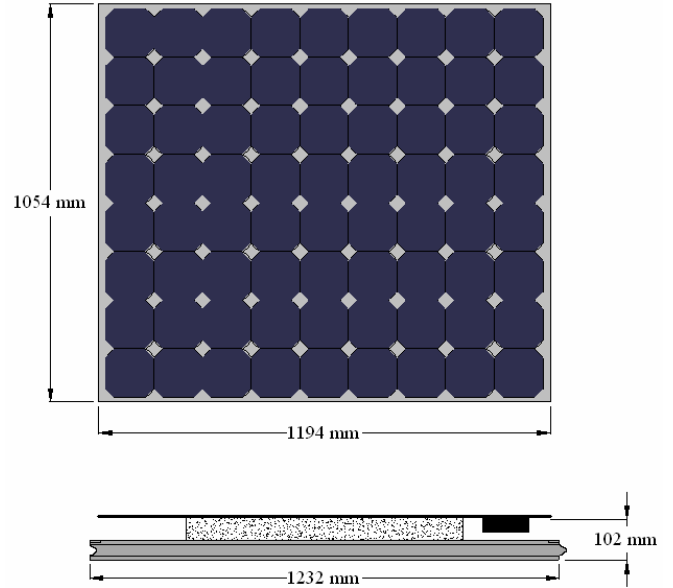


**Figure 2 Photovoltaic Module**

The direct current from the photovoltaic array is converted to three-phase 208 V alternating current by means of a grid-interconnected inverter. In addition to converting direct to alternating current, the inverter incorporates control logic that forces the photovoltaic array to operate at or near its maximum power point as well as providing several safety features. For example, if utility power is lost, the inverter automatically disconnects the photovoltaic system from the utility grid preventing the flow of electrical power into a possibly damaged grid system. Finally, a transformer is used to increase the 208 V output from the inverter to 480 V, the distribution voltage used within NIST facilities.

**Table 1 – PV Module and System Array Specifications**

PV Module	Stabilized Power = 150 W dc Open Circuit Voltage = 43.4 V Voltage at Peak Power = 34.0 V Short Circuit Current = 4.8 A Current at Peak Power = 4.4 A Dimensions = 1054 mm x 1194 mm
PV Array	No. of Modules in Series-Wired String = 13 No. of Parallel Strings in Source Circuit = 18 No. of Source Circuits = 1 Total Number of Modules = 234 Stabilized Power = 35 kW dc Open Circuit Voltage = 564 V Voltage at Peak Power = 442 V Short Circuit Current = 86 A Current at Peak Power = 79 A

The manufacturer of the rooftop photovoltaic system installed a data acquisition system to measure ambient temperature, solar radiation, wind speed, and electrical power delivered to the grid. A silicon photovoltaic sensor provides the radiation measurement. Data is captured each minute and average or integrated, as appropriate, over 15 min intervals. The amount of storage available for the 1 min and 15 min data is limited to approximately 2 h and 2 weeks, respectively.

On the rooftop of an adjacent building, NIST researchers maintain a separate meteorological station [4]. This meteorological station includes two precision spectral pyranometers (PSPs) that measure global horizontal radiation. From the start, the radiation measurements made using the manufacturer's supplied silicon photovoltaic sensor and the meteorological station's PSPs differed significantly. To help understand the cause of the discrepancy, four PSPs were installed in close proximity to the rooftop photovoltaic array. The outputs from these four pyranometers were measured and recorded by a separate data acquisition system every five minutes. This separate data acquisition system became operational in February 2002.

Prior to their deployment near the rooftop photovoltaic array, the four PSPs were placed next to the meteorological station's pyranometers for several days. The calibration factor for each of the four PSPs was adjusted slightly in an effort to match readings with one of the meteorological station's PSPs. The five PSPs agreed to within 2 % of each other prior to adjusting the calibration coefficients. This procedure allowed direct comparisons between the solar radiation measured at the rooftop photovoltaic system versus the meteorological station.

### VARIATION IN RADIATION MEASUREMENTS

A review of the photovoltaic system's performance one month after start-up revealed that the solar insolation measured at the array was substantially higher than the insolation recorded at the nearby meteorological station. Comparing the November 2001 total horizontal solar insolation values, for example, the manufacturer's supplied sensor recorded 95.5 kW h/m<sup>2</sup> versus 75.7 kW h/m<sup>2</sup> recorded by the meteorological station's PSP, a 26 % difference. In order to rule out an instrumentation error, a precision spectral pyranometer was placed in close proximity to the manufacturer's silicon photovoltaic sensor.

During a limited comparison period, the manufacturer's sensor agreed within 3.6 % of the pyranometer's reading. This agreement was well within the 5 % accuracy stated by the manufacturer<sup>1</sup> of the silicon photovoltaic sensor [5]. Both the precision spectral pyranometer and the photovoltaic system's sensor recorded readings approximately 26 % greater than those recorded at the meteorological station. It was concluded that the large differences were not attributable to measurement

<sup>1</sup> Certain trade names and company products are mentioned in the text or identified in an illustration in order to adequately specify the experimental procedure and equipment used. In no case does such an identification imply recommendation or endorsement by the National Institute of Standards and Technology, nor does it imply that the products are necessarily the best available for the purpose.

errors but most likely due to reflections from the Administration Building's tower.

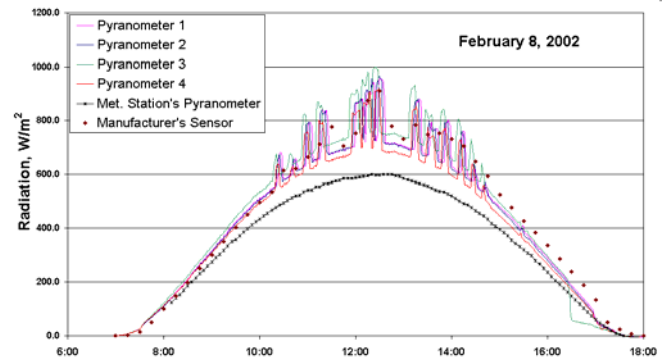


**Figure 3 Solar Radiation Measurement Comparison**

During the month of February 2002, four precision spectral pyranometers became available and were used to further explore discrepancies between the radiation measurements at the photovoltaic array's site and the nearby meteorological station. Initially the four sensors were positioned in close proximity to the manufacturer's sensor. The resulting data for the four pyranometers and the meteorological station's pyranometer are shown in Fig. 3 for a clear day (February 8, 2002). Data from the manufacturer's sensor, available every 15 min, are also displayed. The sensors located at the photovoltaic system's site recorded significantly higher values of solar radiation throughout the day. A very interesting phenomenon that occurs is the radiation spikes between 9:45 a.m. and 2:30 p.m. Visual observations on a subsequent day revealed that these solar radiation "spikes" were due to reflections from the vertical aluminum mullions associated with the Administration Building's curtain wall system.

In late March 2002, the four pyranometers were positioned at the four corners of the right photovoltaic sub-array as shown in Fig. 1. Figure 4 displays the monthly incident solar radiation measured by the manufacturer's sensor, the meteorological station's pyranometer and, com-

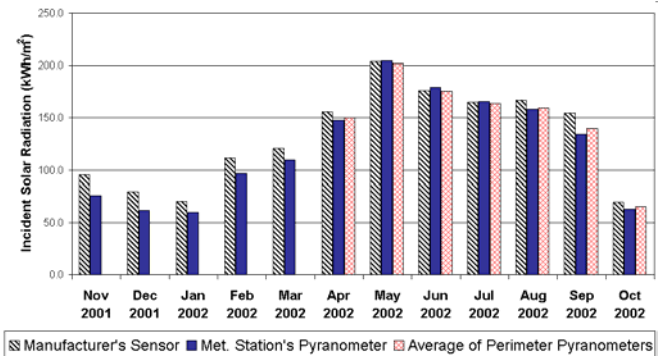


**Figure 4 Monthly Incident Solar Radiation**

mencing April 2002, the average of the four pyranometers. A comparison between the manufacturer's sensor and the meteorological station's pyranometers reveals an interesting trend. During the first 5 months, the solar radiation values recorded at the two locations differ by a significant amount. However, during the months of May, June and July, the readings at the two locations are in excellent agreement. During the months of August, September, and October the manufacturer's sensor once again recorded higher values of incident solar radiation. This trend is due to the monthly variation in the sun's elevation. The sun's zenith angle for mid-June at solar noon is 16.2° compared to a zenith angle of 58° for November. The higher zenith angles, of the winter months, cause reflections from the Administration Building's tower and enhanced radiation on the manufacturer's supplied silicon photovoltaic sensor.

### ELECTRICAL PERFORMANCE AND OVERALL SYSTEM EFFICIENCY

The electrical energy delivered by the photovoltaic system to the electrical grid for each billing cycle was computed by summing the 15 min integrated values stored within the data acquisition system. Table 2 lists the monthly billing cycles and the energy supplied by the photovoltaic system. The efficiency of the solar photovoltaic system, including inefficiencies associated with the DC to AC inverter and the step-up transformer, in converting the incident solar energy into electrical energy delivered to the grid is computed using:

$$\eta_c = \frac{\int_{\tau_1}^{\tau_2} P \, d\tau}{A \int_{\tau_1}^{\tau_2} H_T \, d\tau} \quad (1)$$

where

- $A$  is a representative area,  $m^2$ ,
- $H_T$  is the global incident solar radiation,  $W/m^2$ ,
- $P$  is the system's alternating current electrical power output,  $W$

and  $\tau_1$  and  $\tau_2$  correspond to the beginning and end of each billing cycle

The selection of an appropriate area and the source of the radiation measurement for computing the efficiency are somewhat subjective. Three different areas are used to present the efficiency results – cell area, module area, and footprint area. The cell area is the total number of active photovoltaic cells times the area of a single cell. The module area is defined as the glazed area of a single photovoltaic module times the number of electrically interconnected modules. Finally, the footprint area represents the total area of the roof installation, including the inactive modules, the perimeter curbing system, and the electrical interconnect boxes on the roof. The footprint area does not include the unoccupied space between the left and right arrays. The incident radiation measurement selected for computing the conversion efficiencies is also a subjective choice. At least three different choices are available – the radiation measurement provided by the silicon manufacturer's

photovoltaic sensor, the meteorological station's precision spectral pyranometer or the average value measured by the four precision spectral pyranometers at the site of the photovoltaic installation.

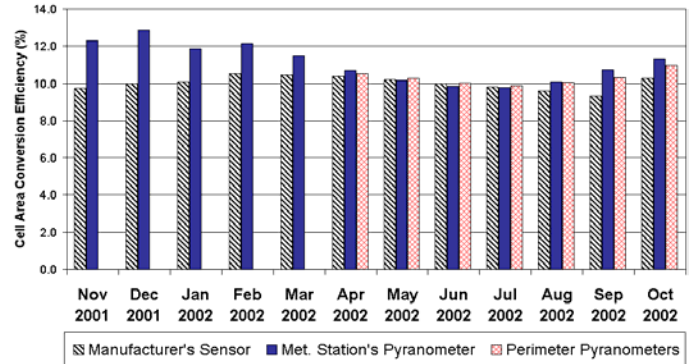


Figure 5 Cell Area Conversion Efficiencies

Use of the manufacturer's sensor provides efficiency results that are available to the typical system owner. However, in this particular installation, the Administration Building's tower causes reflections on the manufacturer's sensor and a portion of the photovoltaic array. During time intervals in which solar radiation is reflected from the adjoining building tower, the efficiencies computed using the manufacturer's supplied sensor would be lower than efficiencies computed using radiation data from the meteorological station. The average value measured by the four precision pyranometers, during these time intervals, will yield higher efficiency results than those computed using the manufacturer's sensor and lower efficiencies than those computed using the meteorological station's pyranometer.

The measured efficiency results for the photovoltaic system are given in Table 2. For each month the efficiencies are presented using cell, module, and footprint areas. For a given area, efficiencies are computed using solar radiation values measured by the manufacturer's sensor, the meteorological station's pyranometer, and the four pyranometers positioned around the photovoltaic array's perimeter. These efficiencies are respectively labeled as Manufacturer, Meteorological, and Perimeter in Table 2. Unlike module efficiencies reported at standard rating conditions, the Table 2 results include the effects of elevated operating temperature, the varying incident angle between the modules and sun, varying meteorological conditions, module soiling, and inverter and step-up transformer inefficiencies.

**Table 2 – NIST Photovoltaic System Performance**

Billing Period	Delivered Energy (kWh)	Conversion Efficiencies								
		Cell Area			Module Area			Footprint Area		
		Manufacturer's Sensor	Meteorological	Perimeter	Manufacturer's Sensor	Meteorological	Perimeter	Manufacturer's Sensor	Meteorological	Perimeter
Nov 01	2220.7	9.7	12.3	-	8.0	10.1	-	6.7	8.4	-
Dec 01	1896.2	10.0	12.9	-	8.2	10.6	-	6.9	8.9	-
Jan 02	1685.5	10.1	11.9	-	8.3	9.7	-	6.9	8.2	-
Feb 02	2800.1	10.5	12.2	-	8.6	10.0	-	7.2	8.4	-
Mar 02	3016.5	10.5	11.5	-	8.6	9.4	-	7.2	7.9	-
Apr 02	3777.6	10.4	10.7	10.5	8.5	8.8	8.6	7.1	7.4	7.2
May 02	4951.0	10.2	10.2	10.3	8.4	8.3	8.4	7.0	7.0	7.1
Jun 02	4202.5	10.0	9.8	10.0	8.2	8.1	8.2	6.9	6.8	6.9
Jul 02	3860.5	9.8	9.8	9.9	8.1	8.0	8.1	6.7	6.7	6.8
Aug 02	3826.0	9.6	10.1	10.1	7.9	8.3	8.3	6.6	6.9	6.9
Sep 02	3439.6	9.3	10.7	10.3	7.7	8.8	8.5	6.4	7.4	7.1
Oct 02	1702.0	10.3	11.3	11.0	8.4	9.3	9.0	7.1	7.8	7.5
Overall	35676.1	10.0	10.8	10.2	8.2	8.8	8.4	6.9	7.4	7.0

NOTE: Cell Area - 238.686 (m<sup>2</sup>); Module Area - 290.85 (m<sup>2</sup>); Footprint Area - 347.269 (m<sup>2</sup>)

Efficiencies, computed using the cell area, are plotted for each month, using radiation measurements from the three available sources, Fig. 5. During the months that a large amount of solar radiation is reflected due to the high zenith angles (November 2001 - March 2002 and August 2002 - September 2002), efficiencies based on the manufacturer's sensor are significantly less than the efficiencies computed using the sensor. Based on the solar radiation measurements from the meteorological station, the overall conversion efficiencies for the entire monitoring period based on cell, module, and footprint areas are 10.8 %, 8.8 %, and 7.4 %, respectively.

**ECONOMIC SAVINGS**

The total installed cost of the photovoltaic system, including the manufacturer's supplied data acquisition system, was \$239 945 or \$6.86 per DC watt at standard rating conditions. The photovoltaic system reduces NIST's electric utility bill by displacing electrical energy that would have been purchased and by lowering the site's peak electrical demand. The electric utility's energy and demand charges for large commercial customers like NIST, Table 3, are divided into summer billing months (June-October) and winter billing months (November- May). Within a given billing month the charges are divided into distribution, transmission, and generation. The energy generation service charges are further divided into on-peak (12 p.m. to 8 p.m.), intermediate-peak (8 a.m. to 12 p.m.) and off-peak (12 p.m. to 8 a.m.) time intervals. The cost associated with a kWh of electricity can range from 4.85 cents during summer on-peak hours to a low of 2.29 cents during winter off-peak hours. During both winter and summer months, a maximum peak demand charge is imposed based upon the maximum 30 min power demand. During summer billing months, a second "on-peak" demand charge is assessed. This charge is based on the maximum 30 min demand recorded during the on-peak (12 p.m. to 8 p.m.) time interval. The maximum demand charge, including distribution, transmission, and generation is currently \$4.07 per kW. The additional summer month on-peak demand charge is \$9.88 per kW.

**Table 3-NIST Electric Utility Billing Schedule**

	Summer Billing Jun-Oct		Winter Billing Nov-May	
<b>Distribution Service Charge</b>				
Customer	\$275.67	per mo	\$275.67	per mo
Kilowatt-hour Charge	0.590¢	per kwhr	0.590¢	per kwhr
Kilowatt Charge				
On Peak	\$1.7738	per kw		
Maximum	\$0.7350	per kw	\$0.7350	per kw
<b>Transmission Service Charge</b>				
Kilowatt-hour Charge	0.265¢	per kwhr	0.265¢	per kwhr
Kilowatt Charge				
On Peak	\$0.7154	per kw		
Maximum	\$0.2940	per kw	\$0.2940	per kw
<b>Generation Service Charge</b>				
Kilowatt-hour Charge				
On Peak	3.994¢	per kwhr	3.265¢	per kwhr
Intermediate	3.323¢	per kwhr	2.708¢	per kwhr
Off Peak	1.745¢	per kwhr	1.438¢	per kwhr
Kilowatt Charge				
On Peak	\$7.390	per kw		
Maximum	\$3.040	per kw	\$3.040	per kw
NOTE:	On Peak (12 PM to 8 PM) Intermediate (8 AM to 12 PM) Off Peak (12 AM to 8 AM)			

Electrical energy and power demand savings attributable to the photovoltaic system are given in Table 4 and Fig. 6 for each billing period. The savings associated with the energy displaced by the system is computed by multiplying the sum of the distribution, transmission, and generation charges, for the appropriate time interval, by the quantity of energy produced by the photovoltaic system during that time interval. The reduction in peak demand charges attributable to the photovoltaic system are computed in the following manner. The date and time at which the maximum peak demand and, during the summer billing months, the on-peak demand charges occur are obtained from the electricity utility. The

power output of the photovoltaic system during the utility's maximum peak demand and on-peak demand periods is obtained from the archived system performance data and subsequently multiplied by the sum of the appropriate distribution, transmission, and generation peak demand charges.

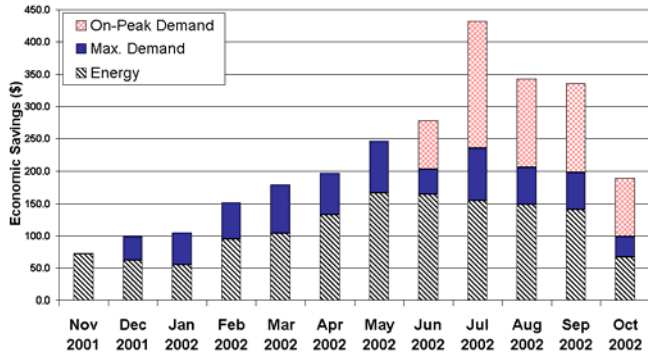


**Figure 6 Economic Savings Associated with Solar Photovoltaic System**

It is interesting to note, Fig. 6, that savings attributable to reducing NIST's power demand on the electric utility represents a significant fraction of the total economic savings associated with the photovoltaic system. In fact, during the months of July, August, and September 2002, the peak demand savings far exceed the energy displaced savings!

The 51 mm thick extruded insulation to which each PV module is laminated provides additional thermal insulation, approximately 1.76 m<sup>2</sup>·K/W (R-10 °F·ft<sup>2</sup>·h/Btu), to the portion of the Administration Building's roof occupied by the photovoltaic modules. The roof's original thermal resistance is assumed to be 4.05 m<sup>2</sup>·K/W (R-23.0 °F·ft<sup>2</sup>·h/Btu) [6]. This additional insulation reduces heat gains during months in which cooling is required and heat losses during months in which heating is required. The difference in heat transfer through the roof area occupied by the photovoltaic modules for each month was computed using the following equation,

$$Q = A \left[ \frac{1}{R_o} - \frac{1}{R_{PV}} \right] \int_0^\tau (t_o - t_a) d\tau \quad (2)$$

where

- t<sub>o</sub> is the outdoor ambient temperature measured using the manufacturer's supplied sensor, °C (°F)
- t<sub>a</sub> is the 21.7 °C (77 °F) assumed indoor ambient temperature
- A is the area of the roof occupied by the photovoltaic modules, m<sup>2</sup> (ft<sup>2</sup>)
- R<sub>o</sub> is the thermal resistance of the original roof, 4.05 m<sup>2</sup>·K/W (R-23.0 °F·ft<sup>2</sup>·h/Btu)
- R<sub>PV</sub> is combined thermal resistance of the original roof and the PV system's insulation, 5.81·m<sup>2</sup>·K/W (R-33 °F·ft<sup>2</sup>·h/Btu).

and τ is the number of hours within each month (h).

During months that cooling was required, the economic savings was computed by taking the difference between the

heat gain associated with the original and enhanced roof section, dividing by the estimated overall efficiency of the mechanical chillers and associated distribution equipment [6], and finally multiplying by the appropriate electrical energy cost. The savings incurred during the heating season is computed by taking the difference between the heat loss associated with the original and enhanced roof, dividing by the estimated efficiency of the boilers and associated distribution equipment [6], and multiplying by the cost of natural gas used to fuel the boilers.

The savings attributed to the enhanced thermal insulation provided by the photovoltaic system are listed in Table 4. The monthly savings range from \$0.16 during the month of September 2001 to a high of \$9.57 computed for the month of December 2001. The total savings due to the additional thermal insulation, \$49.83, is small in comparison to the displaced energy savings and peak demand reductions listed in Table 4. The small savings is partially attributable to the fact that the original roof was reasonably well insulated.

**Table 4 Economic Savings Associated with Photovoltaic System**

Billing Period	Energy Savings	Max Peak Demand Savings	On-Peak Demand Savings	Thermal Savings	Total Savings
Nov 01	71.49	1.77	-	5.09	78.35
Dec 01	61.43	37.39	-	9.57	108.38
Jan 02	54.47	50.10	-	8.52	113.09
Feb 02	94.84	56.71	-	8.47	160.01
Mar 02	104.19	75.28	-	6.56	186.03
Apr 02	132.77	63.33	-	3.17	199.27
May 02	166.18	79.92	-	1.66	247.75
Jun 02	164.24	38.40	75.95	0.60	279.19
Jul 02	154.17	81.12	196.95	0.87	433.12
Aug 02	148.62	56.71	137.68	0.81	343.81
Sep 02	140.58	56.97	138.31	0.16	336.02
Oct 02	67.35	31.09	90.14	4.35	192.92
Total \$	1360.32	628.76	639.03	49.83	2677.94

### ENVIRONMENTAL IMPACT

The fuel mix of the electric utility providing service to the NIST site consists of 28.2 % coal, 12.7 % gas, 30 % nuclear, and 28 % oil [7]. Renewable energy sources account for approximately 1 % of the current fuel mix. According to the utility [7], the quantity of sulfur dioxide, nitrogen oxides, and carbon dioxide associated with each megawatt hour (MWh) of electricity is approximately 4.8 kg, 1.4 kg, and 529 kg. Since November 1, 2001, the photovoltaic system has generated 35.7 MWh of electricity during its eleven months of operation. It is anticipated that the system will provide 1071 MWh over its expected 30 year life span. Thus, the projected 30 year lifetime avoided emissions for the photovoltaic system, based on the current fuel mix and air emissions per MWh of electricity, are 5141 kg of sulfur dioxide, 1499 kg of nitrogen oxides, and 566.6 t of carbon dioxide.

A second means of estimating the avoided emissions is possible through the use of the Environmental Protection

Agency's (EPA) web based solar calculator that computes emission reductions through the use of various solar technologies [8]. The web site requires that the user select the state in which the photovoltaic system is located and the power output of the photovoltaic array. The solar calculator predicts that 9630 kg of sulfur dioxide, 4020 kg of nitrogen oxide, and 1,579.4 t of carbon dioxide will be avoided during the projected 30 year system lifespan from a 35 kW photovoltaic system in Maryland. The greater emission avoidance values projected by EPA's solar calculator are considerably greater than those projected using the information provided by the utility.

Reasons for the large discrepancies may include the fact that the EPA's solar calculator uses emissions data from all the electric utilities within the state of Maryland and assumes that the photovoltaic panels are tilted towards the sun at an angle that optimizes annual performance. Additionally, the EPA algorithm may also assume a conversion efficiency greater than the actual efficiency of the equipment used in this installation. Finally, it should be noted that neither methodology takes into account the reduced space conditioning loads resulting from the additional thermal insulation associated with the photovoltaic system.

## SUMMARY

A 35 kW roof top photovoltaic system has been installed at the National Institute of Standards and Technology in Gaithersburg, MD. The system became operational on September 14, 2001 and represents NIST's first on-site source of renewable energy. The total installed cost of the system was \$239 945.

During the past year the system has provided 35 676 kWh of electrical energy. In addition to displacing electrical energy that would have been purchased from the electric utility, the system has reduced the site's demand charges. During its first year of operation, the system has saved \$2678. To date, the savings in demand charges are essentially equivalent to savings as a result of displaced energy. Annual savings attributable to the increased thermal resistance associated with the photovoltaic system amounted to \$49.83

Two different techniques were used to estimate the impact that the system will have on the electric utility's emissions. Using data provided by the electric utility, the avoided emissions associated with the system are 5141 kg of sulfur dioxide, 4499 kg of nitrogen oxides, and 566.6 t of carbon dioxide. Using a tool included within EPA's Global Warming website, the projected avoided emissions are 9630 kg of sulfur dioxide, 4020 kg of nitrogen oxide, and 1,579.4 t of carbon dioxide. The large discrepancy between the estimates in avoided emissions is currently being explored.

The area selected and the placement of the instrument used to measure solar radiation can have a significant impact on the reported conversion efficiency of a system. Annual conversion efficiencies of 10.8 %, 8.8 %, and 7.4 % were achieved using cell, module, and footprint areas, respectively. Reflected solar energy, from an adjacent building tower, resulted in computed efficiencies using the manufacturer's supplied radiation sensor significantly less than the

efficiencies computed using a sensor that was not exposed to the reflected solar energy. The amount of reflected radiation, and thus the differences in computed efficiencies, varied based on the solar zenith angle. The greatest differences take place during the winter months when the highest zenith angles occur.

## ACKNOWLEDGEMENTS

The authors would like to express their appreciation to Douglas Elznic, Mark Kuklewicz, and Ralph Whalen of NIST's Plant Division for providing the funding, engineering support, and system installation supervision in order to procure and install the photovoltaic system. The authors are also grateful to Tom Leyden and Lori Mitchell of the Power Light Corporation for providing guidance concerning the use of manufacturer's supplied data acquisition system. Merle Guyton is acknowledged for assisting in the calibration and installation of the solar radiation instruments used in this study. Sincere appreciation is extended to Paula Svincek for manuscript preparation.

## REFERENCES

- [1] Neff, D.E., and Bienkiewicz, B., "Wind Tunnel Study of PowerGuard® RT Arrays," Final Report, PowerLight Corp., Berkeley, CA.
- [2] American Society of Civil Engineers, 7-98. (2000), "Minimum Design Loads for Buildings and Other Structures," Revision of ANSI/ASCE7-95.
- [3] Shell Solar Product Information Sheet, *Shell SP150-P, Photovoltaic Solar Module*, V2/SP150-P/05/02/US.
- [4] Fanney, A.H., Dougherty, B.P., Davis, M.W., 2000, "Building Integrated Photovoltaic Test Facility," *Proceedings of the, Solar 2000: Solar Powers Life, Share the Energy*, Conference, June 16-21, 2000, Madison WI.
- [5] LI-COR Radiation Sensors, <http://env.licor.com/Products/Sensors/rad.htm>.
- [6] Personal communication with Mark Kuklewicz, Plant Division, NIST, December, 2002.
- [7] Pepco-Environment Policy, Air Emissions, [http://www.pepco.com/env\\_mdemis.htm](http://www.pepco.com/env_mdemis.htm).
- [8] EPA Global Warming Site: Renewable Energy – Annual Emissions Avoided in Maryland, "<http://itdomino1.icfconsulting.com/epa/rew/rew.nsf/solar/impact?Open&MD1&1&35&&Photovoltaic>"